Outdoor demonstration-scale flat plate photobioreactor for resource recovery with purple phototrophic bacteria

Tim Hülsen, Christian Züger, Zuo Meng Gan, Damien J Batstone, David Solley, Pip Ochre, Brett Porter, Gabriel Capson-Tojo

Journal Pre-proof

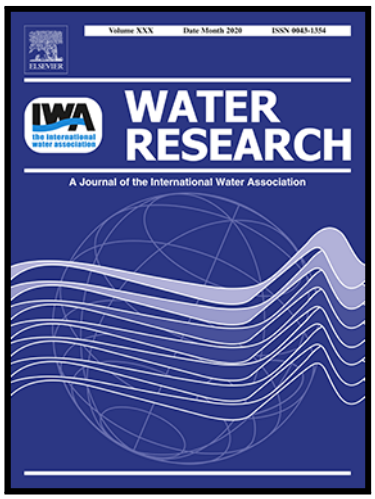

Outdoor demonstration-scale flat plate photobioreactor for resource recovery with purple phototrophic bacteria

Tim Hülsen , Christian Züger , Damien J. Batstone , David Solley , Pip Ochre , Brett Porter , Gabriel Capson-Tojo

PII: S0043-1354(22)00290-1
DOI: https://doi.org/10.1016/j.watres.2022.118327
Reference: WR 118327

To appear in: *Water Research*

Received date: 7 January 2022
Revised date: 17 March 2022
Accepted date: 18 March 2022

Please cite this article as: Tim Hülsen , Christian Züger , Damien J. Batstone , David Solley , Pip Ochre , Brett Porter , Gabriel Capson-Tojo , Outdoor demonstration-scale flat plate photobioreactor for resource recovery with purple phototrophic bacteria, *Water Research* (2022), doi: https://doi.org/10.1016/j.watres.2022.118327

Outdoor demonstration-scale flat plate photobioreactor for resource recovery with purple phototrophic bacteria

Tim Hülsen [a,*] Christian Züger [b], Damien J. Batstone [a], David Solley [c], Pip Ochre [c], Brett Porter [d], Gabriel Capson-Tojo [a,e]

[a] Australian Centre for Water and Environmental Biotechnology, The University of Queensland, Brisbane, QLD 4072, Australia

[b] Eidgenössische Technische Hochschule Zürich (ETH), 8092 Zürich, Switzerland

[c] GHD, Brisbane, QLD 4000, Australia

[d] Inghams Enterprises, Murarrie, QLD 4172, Australia

[e] CRETUS Institute, Department of Chemical Engineering, Universidade de Santiago de Compostela, 15782 Santiago de Compostela, Galicia, Spain

* Corresponding author: tel. +61 7 3346 3214, e-mail: *t.huelsen@awmc.uq.edu.au*

Abstract

To make purple phototrophic bacteria (PPB)-based technologies a reality for resource recovery, research must be demonstrated outdoors, using scaled reactors. In this study, a 10 m long PPB-enriched flat plate photobioreactor (FPPBR) with a volume of 0.95 m^3 was operated for 253 days, fed with poultry processing wastewater. Different operational strategies were tested, including varying influent types, retention times, feeding strategies, and anaerobic/aerobic conditions in a novel mixed metabolic mode concept. The overall results show that regardless of the fermented wastewater fed (raw or after solid removal via dissolved air flotation) and the varying environmental conditions (*e.g.*, light exposure and temperatures), the FPPBR provided effective volatile fatty acids (VFAs), N, and P removals

(average efficiencies of >90%, 34-77%, and 28-45%, respectively). The removal of N and P was limited by the availability of biodegradable COD. Biomass (C, N and P) could be harvested at ~90% VS/TS ratio, 58% crude protein content and a suitable amino acid profile for potential feed applications. During fully anaerobic operation with semicontinuous/day-only feeding, the FPPBR showed biomass productivities between 25-84 g VS m^{-2} d^{-1} (high due to solid influx; the productivities estimated from COD removal rates were 6.0-24 g VS·m^{-2}·d^{-1} (conservative values)), and soluble COD removal rates of up to 1.0 g·L^{-1}·d^{-1} (overall average of 0.34±0.16 g·L^{-1}·d^{-1}). Under these conditions, the relative abundance of PPB in the harvested biomass was up to 56%. A minimum overall HRT of 2-2.4 d (1.0-1.2 d when only fed during the day) is recommended to avoid PPB washout, assuming no biomass retention. A combined daily-illuminated-anaerobic/night-aerobic operation (supplying air during night-time) exploiting photoheterotrophy during the day and aerobic chemoheterotrophy of the same bacteria at night improved the overall removal performance, avoiding VFA accumulation during the night. However, while enabling enhanced treatment, this resulted in a lower relative abundance of PPB and reduced biomass productivities, highlighting the need to balance resource recovery and treatment goals.

Graphical abstract

Flat-plate photobioreactor (FPPBR) with enriched purple phototrophic bacteria (10 m long; 950 L, 20 illuminated m^2, run for 253 days, outdoors)

Fermented wastewater

- **Volatile fatty acid removal >90%**
- **N and P removal limited by bioavailable COD**
- **Up to 84 gVS $m^{-2}d^{-1}$ biomass productivity (corrected without influent solids)**
- **Relative Abundance of PPB up to 0.56**
- **Removal rate up to 1.0 gSCOD L^{-1} d^{-1}**
- **HRT (=SRT) ~1.6-2.4 d**
- **Aeration at night improved the treatment performance**

Keywords

Wastewater; nutrient recovery; purple phototrophic bacteria; PPB; photobioreactor

Highlights

- Long term outdoors operation of a 10 m FPPBR for 253 days
- PPB showed resilience to variable temperature and irradiance
- SCOD removal rate up to 1.0 g·L^{-1}·d^{-1} without biomass retention at HRT ~2 d
- >90% of VFA removal at OLR of ~1.5 g COD·L^{-1}·d^{-1}
- Estimated conservative biomass productivities of 6-24 g VS·m^{-2}·d^{-1}

Acronyms

Anammox	Anerobic ammonium oxidation
AM	Acetoclastic methanogens
ASV	Amplicon sequence variant
Att.	Attached
BChl	Bacteriochlorophyll

ChAerD	Chemoheterotrophic growth under aerobic, dark, conditions
COD	Chemical oxygen demand
Cont.	Continuous
CP	Crude protein
DAF	Dissolved air flotation
DNA	Deoxyribonucleic acid
DO	Dissolved oxygen
FDAF	Fermented DAF effluent
FIA	Flow injection analysis
FID	Flame ionization detector
FPPBR	Flat plate photobioreactor
FWW	Fermented wastewater
GC	Gas chromatography
HRT	Hydraulic retention time
IC	Internal Circulation
IBC	Intermediate bulk container
ICP-OES	Inductively coupled plasma optical emission spectroscopy
NIR	Near infrared
OLR	Organic loading rate
PBR	Photobioreactor
PHA	Polyhydroxyalkanoates
PhAnI	Photoheterotrophic growth under illuminated, aerobic, conditions
PLC	Programmable logic controller
PPB	Purple phototrophic bacteria
PVC	Polyvinyl chloride
SCOD	Soluble chemical oxygen demand
SCP	Single-cell protein

SRT	Solids retention time
Susp	Suspended
T	Temperature
TCOD	Total chemical oxygen demand
TKN	Total Kjeldahl nitrogen
TP	Total phosphorus
TS	Total solids
UASB	Upflow anaerobic sludge blanket
UV-VIS	Ultraviolet-visible spectra
VFA	Volatile fatty acid
VS	Volatile solids
3MPPB	Mixed metabolic mode of operation

1. Introduction

Purple phototrophic bacteria (PPB) have reappeared recently as a potential mediator for resource recovery from wastewater, transforming its constituents into single cell proteins (SCP) and several other products, such as polyhydroxyalkanoates (PHA), hydrogen, carotenoids, or fertilizers (Capson-Tojo et al., 2020). Recent literature has exploited their anaerobic photoheterotrophic metabolism, which enables simultaneous removal and recovery of organics, nitrogen and phosphorus at biomass yields close to 1.0 g $COD_{biomass}$·g $COD_{removed}^{-1}$ (COD being chemical oxygen demand) (Capson-Tojo et al., 2020).

High biomass yields during photoheterotrophic growth are enabled by the utilisation of light as energy source (*i.e.*, photophosphorylation, and to a lesser extent phosphorylation). PPB use mostly near infrared (NIR) light to drive photoheterotrophic metabolism under anaerobic conditions, a capability almost exclusive to PPB (Saer and Blankenship, 2017). NIR light is harvested via bacteriochlorophylls (BChls) a and b, with maximum absorption peaks between

780 and 1040 nm (Saer and Blankenship, 2017). PPB dominance in photoheterotrophic cultures, artificially illuminated with NIR light for resource recovery, has been proven at lab scale in various reactors for a range of municipal and industrial wastewaters (Hülsen et al., 2018a, 2018b; López-Serna et al., 2019). The incident illumination intensities in these experiments varied between 2.0 and 270 $W \cdot m^{-2}$ (Chitapornpan et al., 2013; Dalaei et al., 2020), with even the lowest intensities being prohibitively expensive when considering a PPB process at scale (Capson-Tojo et al., 2020).

The most logical solution for this challenge is outdoors operation, reducing the capital (for lamps and frames) and operational costs of illumination to zero (due to natural light). Non-NIR wavelengths (*i.e.*, visible or ultraviolet (UV-VIS)) can be eliminated with a low-cost filter. To date, there are only a handful of articles reporting outdoors PPB reactor operation, and most of them did not focus on wastewater treatment or nutrient recovery, but on the generation of hydrogen and PHA from artificial media (Adessi et al., 2012; Carlozzi et al., 2006; Carlozzi and Sacchi, 2001). While these studies exposed the PPB reactors to changing environmental conditions, they are not relevant to wastewater treatment applications, as artificial media and pure cultures were used. In particular, in wastewater applications, influent contamination results in competition with non-phototrophic heterotrophic microbes. Changing irradiances and temperatures, including day and night fluctuations create very dynamic conditions that are expected to affect the wastewater treatment performance via kinetic, microbial, and metabolic changes as well as chemical and physiological changes due to varying wastewater characteristics. So far, only one study has assessed these factors in PPB outdoors reactors, confirming the feasibility of this approach and the resilience of PPB to changing environmental conditions (Hülsen et al., 2022).

For PPB technology to emerge as a realistic resource recovery alternative, outdoors implementation, at scale, and using real wastewater needs to be tested. A general sense of design parameters including hydraulic retention time (HRT), sludge retention time (SRT), organic loading rate (OLR), as well as influent loads removal rates, removal efficiencies, and

biomass productivities are also required. This is crucial to advance the current infancy of PPB technology to the next level, but also to avoid extrapolating unrealistically high performances from small lab-scale reactors to scaled outdoor photobioreactors (PBRs), as previously experienced with microalgae (Richardson et al., 2014). Sensationalised productivities from the lab in algae systems (*e.g.*, 60 $g \cdot m^{-2} \cdot d^{-1}$ or 220 $tonnes \cdot ha^{-1} \cdot d^{-1}$ (National-Research-Council, 2012)) attracted major interest and investment that could not be translated into the field, at least not as annual daily average performance. This is because photosynthetic efficiencies were lower and culture instabilities and grazers impacted productivities, among several other issues (Day et al., 2017; Taiganides, 1992). These problems apply mainly to open ponds, which have lower cost compared with closed PBRs (Benemann et al., 2018). Closed PBRs for microalgae production were deemed too expensive (capital and operational) for wastewater treatment, as production costs generally exceed the relatively low value of the product (Acién et al., 2017).

The main challenge in PPB reactor research is to identify an economic reactor design which allows reasonable translation of laboratory research, and hence avoids the issues which have hindered uptake of algae systems. This requires testing of PBRs in field-relevant conditions early in the technology cycle, preferably using natural light. The metabolic diversity of PPB (and mixed culture communities) in addition offers the opportunity to operate photoheterotrophically at anaerobic, illuminated conditions during the day (PhAnI), and chemoheterotrophically under aerobic, dark conditions during the night (ChAerD). To the best of our knowledge, this mixed metabolic mode (3M) concept with PPB, named 3MPPB, has not been tested to date. Both metabolic modes (PhAnI and ChAerD) have been studied separately, with PPB rapidly outcompeted by non-phototrophic aerobes under prolonged continuous aeration (Capson-Tojo et al., 2021). However, regular metabolic mode changes in day/night coupled to anaerobic/aerobic interval changes have not been studied, and might offer the potential to polish or even treat wastewater at night, at the expense of lower nutrient recovery efficiencies and biomass productivities (due to oxidative losses).

This study aims to evaluate the performance of a 10 m long, 950 L, outdoor PPB flat plate photobioreactor (FPPBR) for resource recovery from poultry processing wastewater. For this purpose, a scalable, modular FPPBR was operated for 253 days, exposed to naturally varying environmental conditions. Various design and operational aspects were tested (*e.g.*, HRT, OLR, feeding regimes, etc.) to optimise the treatment performance and biomass productivities. Large quantities of PPB biomass were harvested to enable the value evaluation of the SCP product. Finally, the possibility of aerating at night in a mixed metabolic mode system (3MPPB) was assessed.

2. Material and methods

2.1. Wastewater origin, pretreatments, and characteristics

Poultry-processing wastewater from a poultry-processing facility in Brisbane (Australia) was used as feed. The system was installed on-site, pumping the wastewater directly from its source (grit trap outlet). The raw wastewater was a mixture of water streams resulting from feather removal, bird degutting and general cleaning. Due to the high solid contents in the raw wastewater, solids accumulated at the bottom and the top of the pilot feed tank (a 1000 L intermediate bulk container; IBC), which resulted in substantial variations in wastewater characteristics. Because of this issue, after Phase I the feed was subsequently taken from the outlet of the primary dissolved air flotation (DAF) unit (no polymers or flocculants were used). The DAF effluent was fermented in the feed tank to improve the bioavailability of organic matter and nutrients for the PPB. Table 1 presents the characteristics of the streams and shows a considerable increase of volatile fatty acids (VFAs), NH_3^+-N, and PO_4^{3-}-P after fermentation. The data also show substantial fluctuations of all measured components. A more extensive characterisation of the raw wastewater, the DAF effluent, and the fermenter effluent, as well as the variations of their compositions over time, can be found in the supplementary material (Table S1 and Figures S1-S3).

Table 1. Raw wastewater, DAF and fermenter effluent characteristics concentrations. Standard deviations are presented in parenthesis.

	Units	Raw wastewater	DAF effluent*	Fermenter effluent**
TCOD	$mg \cdot L^{-1}$	4,288 (1,207)	1,916 (711)	1,976 (584)
SCOD	$mg \cdot L^{-1}$	1,826 (313)	1,045 (343)	1,064 (350)
VFA-COD	$mg \cdot L^{-1}$	68 (47)	122 (87)	513 (324)
TS	$mg \cdot L^{-1}$	2,992 (877)	1,486 (679)	1,553 (608)
VS	$mg \cdot L^{-1}$	2,192 (599)	960 (505)	903 (533)
TKN_{total}	$mg \cdot L^{-1}$	232 (74)	124 (47)	132 (34)
$TKN_{filtered}$	$mg \cdot L^{-1}$	158 (23)	94 (30)	105 (24)
NH_4^+-N	$mg \cdot L^{-1}$	14 (5.4)	21 (12)	75 (31)
TP_{total}	$mg \cdot L^{-1}$	40 (13)	25 (11)	29 (7.4)
$TP_{filtered}$	$mg \cdot L^{-1}$	30 (8.4)	20 (9.1)	23 (5.7)
PO_4^{3-}-P	$mg \cdot L^{-1}$	25 (9.3)	19 (8.5)	22 (5.9)

* DAF effluent was the fermenter influent, and fermenter effluent was the FPPBR influent.

** Excludes Phases I and II data,

TCOD stands for total chemical oxygen demand, DAF for dissolved air flotation, SCOD for soluble chemical oxygen demand, VFA for volatile fatty acid, TS for total solids, VS for volatile solids, TKN for total Kjeldahl nitrogen and TP for total phosphorus.

2.2. Flat plate photobioreactor (FPPBR) set-up

Depending on the operational phase, either raw wastewater or DAF effluent was used as feed to the FPPBR. As noted above, the feed was fermented in an IBC, with a volume of 1 m^3. The fermenter was operated continuously, at an HRT of 1 d, and mixed intermittently (15 minutes every 2 h) via internal liquid recycle provided by a positive displacement pump (Mono CP25, NOV Australia Pty Ltd., Victoria, Australia; 25 $L \cdot min^{-1}$). The same pump model was used to transfer raw wastewater to the IBC. The high level in the fermenter was maintained via an overflow at the top and the bottom (via a standpipe) of the container. The FPPBR was fed from the fermenter, using a positive displacement pump (Mono CP11, NOV Australia Pty Ltd., Victoria, Australia; 11 $L \cdot min^{-1}$).

The FPPBR consisted of 8 modules made from 15 mm clear acrylic. The modules were 1220

mm x 1220 mm x 80 mm (L x H x W). Intermediate modules were jointed by O-rings, while terminal modules had a single closed end. The total length was 9.8 m, with a volume of 953 L, and operated at a working volume of 900 L. The illuminated surface to volume ratio was 21 $m^2 \cdot m^{-3}$. To reinforce the acrylic, and to avoid hydraulic distortion, galvanized steel U-frames (L x W x H: 50 x 50 x 130 mm) were placed at regular intervals along the FPPBR. These were bolted across the top to set parallel geometry. A plastic roof with a slope of 45º was placed on top of the steel bars to avoid contamination. The roof was later changed (due to a storm) to a foam sheet cover. Neither cover provided a gastight seal, hence the reactor was open to the atmosphere. The reactor walls, bottom, and roof were covered with an UV-VIS absorbing foil (Lee filter ND 1.2 299) to limit light input from non-NIR wavelengths. A schematic representation of the treatment train, including the DAF unit, the fermenter, and the PBR, as well as two pictures of the plant are shown in Figure 1.

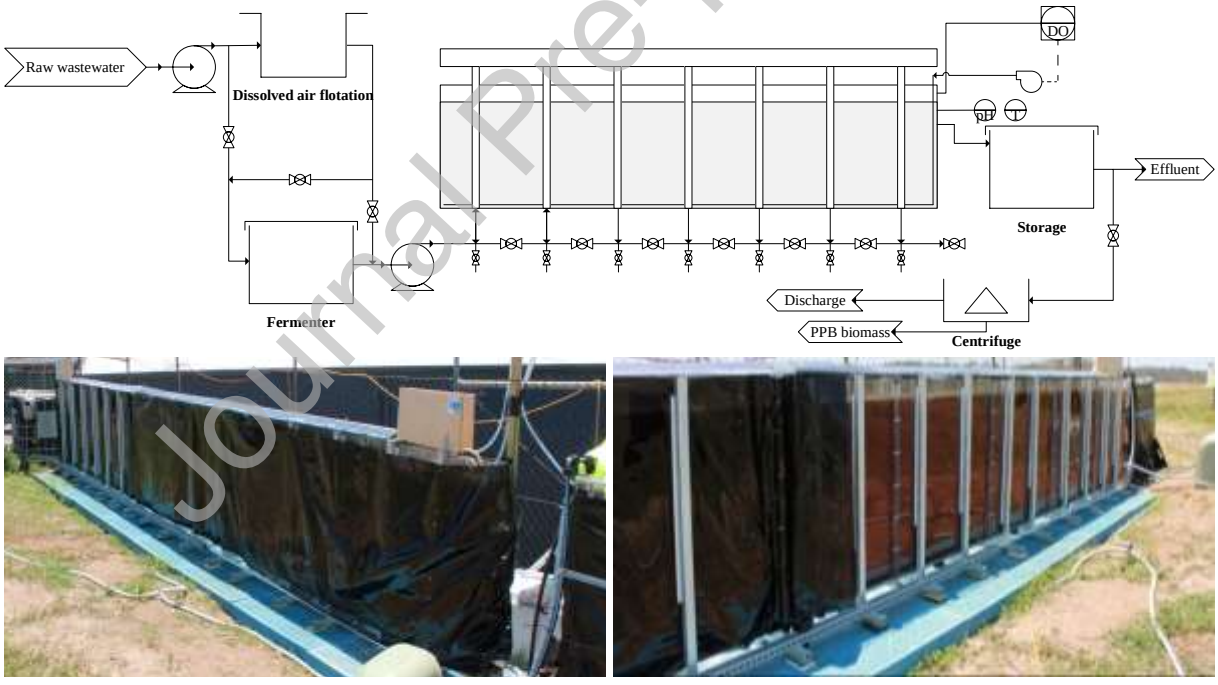

Figure 1. Schematic representation of the treatment plant (top) and pictures of the plant with and without the UV-VIS absorbing foil (bottom).

Each module had a ball valve at the base for feed, drain, and sampling. Feed was provided

via the bottom of the first two modules. Reactor mixing was achieved with a liquid recycle of 7.5:1 $m^3 \cdot m^{-3}$, and a hydro-mechanical mixing device was also tested (protected intellectual property).

The pH, temperature (T), and dissolved oxygen concentration (DO; only from Phase VI on, under aeration) were measured continuously using a Mettler-Toledo M200 transmitter coupled to an Easysense pH 31 sensor and an Easysense O2 21 probe (Mettler-Toledo Limited, Port Melbourne, Australia). As of Phase VII, the DO was controlled using a PLC with an on-off controller connected to a compressor (62.3 $L \cdot min^{-1}$). During Phase VI the aerator was a perforated PVC tube, which was changed to a series of 90 cm air-permeable rubber aquarium aerators (ASE Rubber series) during Phases VII and VIII.

Effluent from the FPPBR was drained into a second 1.0 m^3 IBC, which in turn was drained by gravity into the raw wastewater grit trap. To harvest biomass, the effluent from this IBC was sent to a centrifuge (IC45-M, Interfil, Australia) at feed flows of 6-10 $L \cdot min^{-1}$.

2.3. Demonstration plant operation

The FPPBR was filled with raw wastewater to start the system (composition shown in Hülsen et al. (2022)). No inoculum was used. Once purple colour developed (~3-5 d), ~90% of the reactor volume was drained and topped up with fresh raw wastewater. This was repeated 4 times over ~2 weeks to achieve an intense purple colour. The plant operation was divided into 8 phases, which are detailed in Table 2. Along the 253 days of operation, the main changes included a change from raw wastewater to DAF effluent (after Phase I), from attached to suspended biomass growth (after Phase II), from continuous (day and night feeding) to daytime-only feeding (after Phase IV), from strict anaerobic operation to aeration at night (after Phase V), and testing different aeration strategies during the night (Phases VI-VIII). The change to daytime feeding essentially reduced the HRT by half, because the influent was only pumped during daytime. During Phases VI to VIII, the daytime HRT ranged between 0.80 and 1.05 d, while the total HRT increased to 2.1 and 1.6 d (no feeding at night). The reactor was not mixed at night except when aerated.

Table 2. Operational conditions of the PBR and environmental conditions during the different phases with standard deviation in parenthesis.

Parameter	Phase I	Phase II	Phase III	Phase IV	Phase V	Phase VI	Phase VII	Phase VIII
Duration (d)	1-32	35-60	63-95	93-118	120-127	130-192	195-215	218-253
Substrate	FWW	FDAF	FDAF	FDAF	FDAF	FDAF	FDAF	FDAF
Feeding strategy	Cont.	Cont.	Cont.	Cont.	Daytime	Daytime	Daytime	Daytime
Aeration	No	No	No	No	No	Yes; (perforated PVC)	Yes; Control (fine bubble)	Yes; Control (fine bubble)
HRT (d)*	4.4-5.7	2	2	1	2.4	2.1	2.1	1.6
Growth strategy	Susp.	Att.	Susp.	Susp.	Susp.	Susp.	Susp.	Susp.
Average temperature inside reactor (ºC)**	26 (2.8)	25 (3.5)	25 (3.1)	24 (3.0)	18 (1.5)	16 (1.3)	21 (3.6)	26 (3.3)
Daily average irradiance ($MJ \cdot m^{-2}$)	26 (5.7)	20 (7.9)	19 (7.1)	18 (4.1)	15 (2.3)	13 (1.7)	18 (5.0)	22 (3.7)

FWW stands for fermented wastewater, FDAF for fermented dissolved air flotation effluent, HRT for hydraulic retention time, cont. for continuous, susp. for suspended, and att. for attached. Phase I: fed continuously with FWW; Phases II-III: influent changed to FDAF; Phase IV: HRT decreased to 1 d; Phase V: HRT increased to 2.4 d and feeding only during daytime; Phases VI-VIII: aeration provided during night-time.

* Note that when feeding only during daytime, the daytime (effective) HRT is half of the given value.

** These values correspond to the moments when the samples were taken (10-12 am). Temperature profiles can be found in the supplementary materials.

2.4 Sampling and analysis.

Grab samples of the raw wastewater, DAF effluent, fermenter effluent, the FPPBR content (and occasionally FPPBR effluent) were generally taken twice a week (Monday and Thursday), between 10 am and 12 am. The samples were immediately placed in a cooling box with ice before storage at -20 ºC. Samples were analysed for total COD (TCOD), soluble

COD (SCOD), VFAs, NO_2^--N, NO_3^--N, NH_4^+-N, PO_4^{3-}-P, total Kjeldahl nitrogen (TKN), total phosphorus (TP), total solids (TS), and volatile solids (VS). The efficiency of the mixing system was evaluated by comparing samples from the reactor content (taken after manually mixing the reactor content prior to sampling) with samples of the reactor effluent.

In addition to the samples taken to monitor the FPPBR performance, cycle studies (in Phases II, III, VI, VII, VIII), with a duration of 26-28 h, were conducted to assess day and night trends of TCOD, SCOD, VFA, NH_4^+-N and PO_4^{3-}-P. An auto sampler (ISCO 3700 C Portable Automatic Sampler, RS Hydro, Stoke Prior, England) was set to take a 500 mL sample in varying intervals for different cycle studies (*e.g.*, every hour). The auto sampler was filled with ice to inhibit further activity. The samples were collected the next day using a syringe to take a 50 mL grab sample of the well-mixed 500 mL sample.

2.4. Analytical methods

The concentrations of TCOD and SCOD were determined using COD cell tests (Merck, 1.14541.0001, Darmstadt, Germany). The NH_4^+-N, NO_x-N, NO_2^--N and PO_4^{3-}-P concentrations were measured via flow injection analysis (FIA; QuikChem8000, Hach Company, Loveland, USA). TS and VS were determined as in APHA (2005). The TKN and TP contents were measured by digestion with sulfuric acid, potassium sulphate and copper sulphate as catalysts in a block digestor (Lachat BD-46, Hach Company, Loveland, CO, USA) (Patton and Truitt, 1992). The concentrations of VFAs were measured by gas chromatography (Agilent Technologies 7890A GC System, Santa Clara, CA, USA), using a polar capillary column (DB-FFAP) and a flame ionisation detector (GC/FID). Elemental analysis was performed via inductively coupled plasma optical emission spectrometry (ICP-OES), after sample digestion with 10% nitric acid (Perkin Elmer with Optima 7300 DV, Waltham, MA, USA). The measured soluble compounds were determined after filtration through a 0.45 mm membrane filter (Millipore, Millex®-HP, Merck Group, Darmstadt, Germany). The crude protein (CP) contents in the biomass were estimated from the NH_4^+-N

and TKN contents, according to Eding et al. (2006). Additionally, fat (CF004-1), element (ESI-09 and ESM-05), ash (CF007), protein (CF003-1), and amino acid (CF244) contents of the harvested biomass were determined by Symbio laboratories (method codes in parenthesis) (Eight Mile Plains, QLD, 4113, Australia).

The daily solar irradiance values ($MJ \cdot m^{-2}$) were collected from a local weather station operate by the Australian Bureau of Meteorology, located 2.0 km away from the industrial site (http://www.bom.gov.au/jsp/ncc/cdio/weatherData/av?p_nccObsCode=193&p_display_type=dailyDataFile&p_startYear=&p_c=&p_stn_num=040917).

Inputs are represented as averages and variability in inputs expressed as standard deviation in time-series measurements, represented as $\bar{X}(s_{X_i})$, where $\bar{X}$ is the average value for the data X_i, and s_{X_i} is the standard deviation for the data. Outputs and calculated parameters (including slopes from linear models) are represented as average value, with uncertainty expressed as uncertainty in mean based on a two-tailed *t*-test (95% confidence, 5% significance threshold), represented as $\bar{X} \pm E_{\bar{X}}$, where $E_{\bar{X}}$ is the 95% confidence interval.

2.5. Analysis of the microbial communities

Samples of the reactor content, raw wastewater, and DAF effluent were collected for analysis of the microbial communities. The sample were taken at days 49 (Phase II), 70 (Phase III), 109 (Phase IV), 125 (Phase V), 136, 150, 161, 175, 184, 186 (Phase VI), 208, 218 (Phase VII), and 236, 253 (Phase VIII). These samples were given to the Australian Centre for Ecogenomics for DNA extraction and 16S Amplicon sequencing, using Illumina Miseq Platform. The universal primer pair 926F (50-AAACTYAAAKGAATTGACGG-30) and the 1392wR (50- ACGGGCGGTGWGTRC-30) primer sets were used (Engelbrektson et al., 2010). Trimmomatic was used to trim the raw paired reads, to remove reads shorter that 190 bp and/or with low quality (with a Phred-33 lower than 20) (Bolger et al., 2014). The resulting trimmed paired reads were assembled using PANDAseq, with default parameters (Masella et

al., 2012). The removal of adapter sequences was carried out using the FASTQ Clipper from the FASTX-Toolkit (Pearson et al., 1997). The generated high quality joined sequences were analysed via QIIME v1.8.0 (Caporaso et al., 2010), using the open-reference picking strategy for amplicon sequence variants (ASVs) given by uclust (Edgar, 2010), at 3% phylogenetic distance. Taxonomy was assigned by uclust against the SILVA rRNA database (128_release) (Quast et al., 2013). ASVs with one or two reads were filtered from the ASVs table by command filter_-asvs_from_asv_table.py in QIIME. The ASVs were processed according to Hülsen et al. (2018b).

3. Results and discussion

3.1. Overall performance

3.1.1. Treatment performance

The characteristics of the FPPBR effluent and the removal efficiencies (only based on FPPBR input and output) during the whole operational period are presented in Figure 2 (A - D). The reactor achieved high VFA removal efficiencies in most of the phases (>90%), showing that PPB were able to photoheterotrophically assimilate the VFAs in the wastewater, at rates over 0.5 g SCOD·L^{-1}·d^{-1} (mainly VFA-COD), with peaks up to 1.0 g SCOD·L^{-1}·d^{-1} (Table 3), noting a general VFA-COD limitation. This also indicates that light was not limiting. The process was able to remove all the biodegradable SCOD, leaving a baseline of around 500-700 mg COD·L^{-1}, which was non-degradable (see Figure S3 for the difference between SCOD and VFA-COD in the fermenter) in the given time. This residual, slowly or hardly biodegradable SCOD, was likely composed of complex proteins (keratin residues from feather stream) and lipids (see Section 3.2.2 for a detailed discussion), and will be considered as non-degradable under the given conditions.

The availability of degradable COD in the reactor also determined the N and P removals. PPB have an uptake ratio of around 100:6-10:1-2 COD:N:P (Capson-Tojo et al., 2020; Puyol et al., 2017) and, although the reactor influent had a ratio of 100:6.7:1.5 (see Table 1,

fermenter effluent), the non-degradable COD in the influent led to a lack of organic matter to support complete nutrient uptake. Therefore, the concentrations of N and P in the reactor effluent exceeded common surface water discharge limits (*e.g.*, TN and TP concentrations of 10 and 1.0 $mg \cdot L^{-1}$). The final effluent quality ultimately depends on the wastewater, its COD:N:P ratios, as well as potential pretreatment to adjust the ratios. Additional COD, via dosing (not desired economically) or combining COD rich streams (usually availabe in agri-industrial processes) would improve the treatment performance, removing more of the available N and P (*e.g.*, as $N\text{-}NH_4^+$ and $P\text{-}PO_4^{3-}$). For comparison with other treatment processes, the SCOD, TN and TP removal efficiencies corresponding to the overall plant performance (*i.e.*, including the DAF unit, the fermenter, and the FPPBR) were around 70%, 70% and 50%, respectively (Figure S4). Note, we are not aware of a single biological step that would be able to treat this wastewater as described here. Generally, conventional anaerobic technologies (e.g. Internal ciculation (IC) or upflow anaerobic sludge blanket reactors (UASB)) remove organics (as COD), but no nutrients, and a phosphate precipation step would be required to recover P, while nitrogen would be disspiated as N_2 (e.g. via nitricfication/denitrification, nitritation/denitritation or anaerobic ammonium oxidation (anammox)) in additional downstream processing. Aerobic technologies capture less nutrients compared to PPB mediated systems (e.g. high rate A-stage) where conventional aerobic treatment disspiates up to 97% of the nitrogen as N_2 (via nitrification and denitrification). In any case, various treatment concepts, in a multitank system, would be required to treat this wastewater to the efficiencies given above.

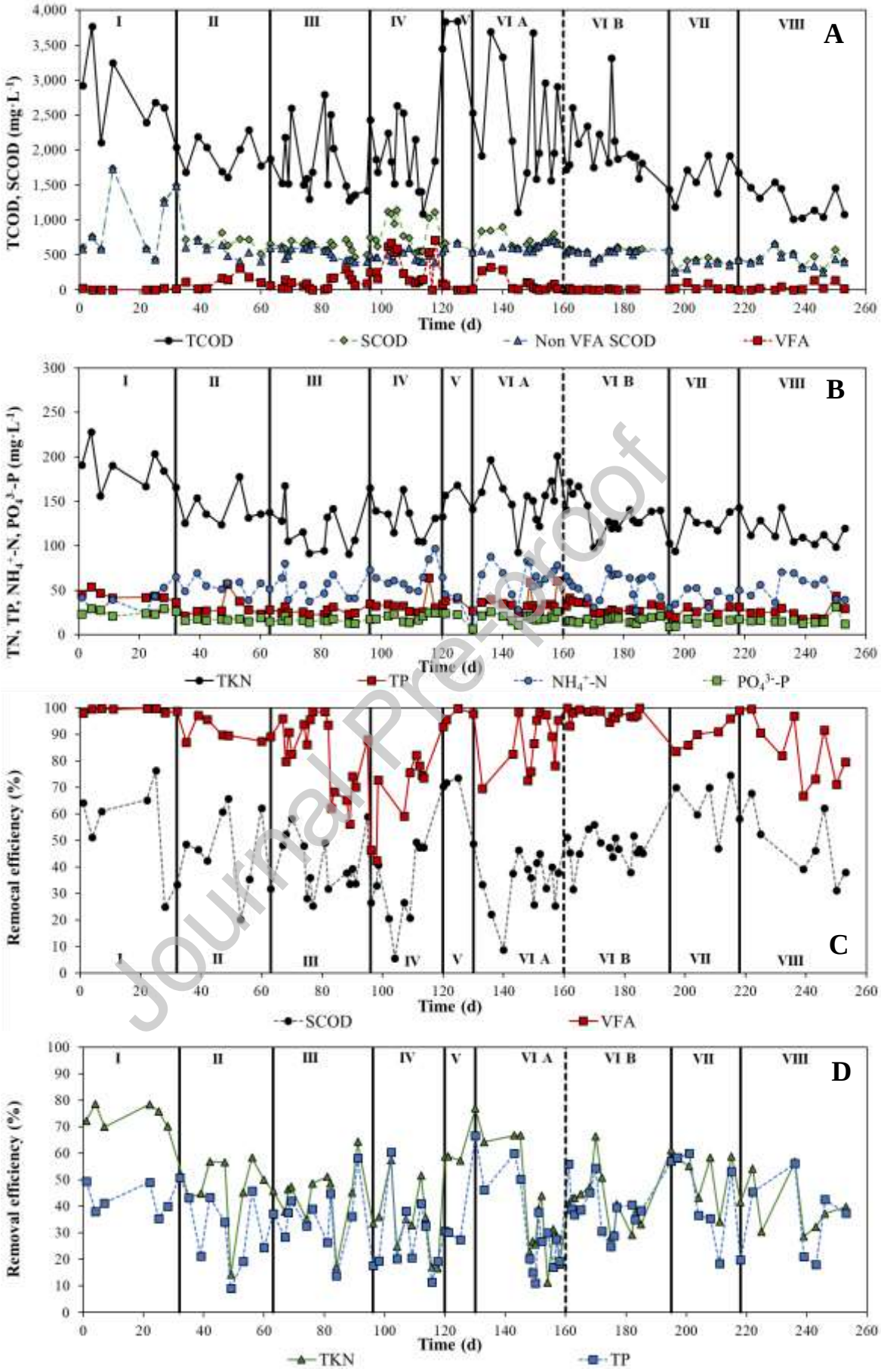

Figure 2. Overall (A,B) effluent concentration of the FPPBR and (C,D) removal efficiencies at the different operational phases. The roman numbers refer to the phases described in Table 2 (Phase I: fed continuously with FWW; Phases II-III: influent changed to FDAF; Phase IV: HRT decreased to 1 d; Phase V: HRT increased to 2.4 d and feeding only during daytime; Phases VI-VIII: aeration provided during night-time).

The removal efficiencies presented in Figure 2 C, D (average values for each phase shown in Table 3) further confirm the lack of bioavailable SCOD for further N and P removal. The VFA removal efficiencies were 85-100% during most of the reactor operation (excluding Phases III and IV). Average SCOD removal efficiencies ranged between 33-72%, with the remaining COD corresponding to the aforementioned non-degradable fraction. The TKN and TP removal efficiencies were between 34-77% and 28-45% respectively. The TKN and TP removal efficiencies shown in Figure 2 D and Table 3 were calculated by comparing the total N and P concentrations in the influent of the FPPBR *vs.* the soluble fractions (rather than the total) in the effluent. The reason for this is that suspended PPB mediated systems do not remove total TKN, TP or COD. Instead, soluble COD, TKN (as NH_4^+-N) and TP (as PO_4^{3-}-P) are assimilated into PPB biomass. Thus, total components will still be measured in the reactor liquid (total removal should be close to zero, due to biomass yields close to unity). NH_4^+-N and PO_4^{3-}-P removal efficiencies were not used because these compounds are both consumed and generated during the treatment process, and therefore do not represent the actual N and P removals in the system. Although this approach might have caused slight overestimations of the removal efficiencies, the presented values are useful to compare operational phases and to estimate the potential performance with effective biomass retention/recovery using off-the-shelf technologies.

Table 3. Average biomass productivities and removal performance of the FPPBR in the different phases (Phase I: fed continuously with FWW; Phases II-III: influent changed to

FDAF; Phase IV: HRT decreased to 1 d; Phase V: HRT increased to 2.4 d and feeding only during daytime; Phases VI-VIII: aeration provided during night-time).

Parameter	Phase I	Phase II	Phase III	Phase IV	Phase V	Phase VI	Phase VII	Phase VIII
Biomass productivity (g TS·m^{-2}·d^{-1})[1]	30±4.1	63±14	61±8.0	75±9.1	126±21	89±14.5	86±18	72±4.1
Biomass productivity (g VS·m^{-2}·d^{-1})[1]	25±3.8	38±12	41±7.2	54±7.4	84±12	59±10	44±15.6	38±3.8
Estimated biomass productivity (g COD·m^{-2}·d^{-1})[2]	9.1±4.0	18.2±10	11.6±3.2	18.7±5.3	38±9.6	11.1±1.2	19.5±10	14.3±5.6
SCOD removal (%)	54±17	48±12.8	40±6.0	33±9.7	72±4.1	39±3.8	67±14	46±11
VFA removal (%)	99±0.7	91±4.5	82±6.7	67±11	96±8.3	91±3.4	87±7.9	85.1±8.7
TKN removal (%)[3]	77±4.2	46±12	45±7.8	34±9.4	58±2.3	30±4.4	53±9.3	37±8.8
TP removal (%)[3]	44±5.7	30±11	37±7.6	28±11	29±4.4	37±16	45±15	34±14
TS content (g·L^{-1})[4]	2.2±0.3	1.3±0.2	1.2±0.2	1.7±0.3	2.5±0.4	1.7±0.3	1.7±0.4	1.5±0.1
OLR (g COD·L^{-1}·d^{-1})	-	1.3±0.3	1.0±0.2	2.2±0.5	1.3±0.3	1.1±0.1	0.8±0.4	0.8±0.3
SCOD removalrate (g·L^{-1}·d^{-1})[4]	0.14±0.06	0.4±0.18	0.20±0.1	0.40±0.1	0.7±0.38	0.2±0.03	0.4±0.24	0.3±0.12
TKN removal rate (mg·L^{-1}·d^{-1})[3]	21±4.5	32±9.4	25±8.2	35±9.6	36±20	27±6.8	25±9.6	22±5.9
TP removal rate (mg·L^{-1}·d^{-1})[3]	2.7±0.8	4.1±1.5	4.3±1.3	7.5±3.4	4.5±1.2	4.8±1.1	5.4±3.5	3.3±2.1

TS stands for total solids, VS for volatile solids, SCOD for soluble chemical oxygen demand, VFA for volatile fatty acid, TKN for total Kjeldahl nitrogen, TP for total phosphorus, TS for total solids, and OLR for organic loading rate. Phase I: fed continuously with FWW; Phases II-III: influent changed to FDAF; Phase IV: HRT decreased to 1 d; Phase V: HRT increased to 2.4 d and feeding only during daytime; Phases VI-VIII: aeration provided during night-time.

[1] Measured including influent solids.

[2] Estimated from the SCOD removed, assuming a PPB photoheterotrophic biomass yields of 1.0 g $COD_{biomass}$·g $COD_{removed}^{-1}$.

[3] Calculated as total nutrient in the influent *vs.* soluble nutrient in the effluent.

[4] This is a conservative approximation for the volumetric biomass productivity (assuming a yield of 1.0 $gCOD_{PPB\text{-}biomass}$ $COD_{removed}^{-1}$).

Despite the variations in the influent characteristics (see Figures S1-S3), and substantial changes in environmental conditions over the operational phases (daily irradiances and temperatures (between 3-32 $MJ \cdot m^{-2}$ and maximum daily temperatures of 14-42 ºC (Figures S5-S6)), the FPPBR performances were reasonably consistent over time (see confidence intervals in Table 3). We also point to significant daily temperatures fluctuations, with day and night temperature fluctuations of up to 24 ºC (Figure S6). The consistency in removal efficiencies and effluent quality proves the resilience of the proposed system (this does not consider daily changes, *e.g.*, day-night cycles).

3.1.2. Resource recovery as biomass

The biomass productivities are shown in Table 3 and Figure 3. In addition to the measured values, a reference biomass productivity was also estimated from the SCOD removed (directly attributable to PPB, and calculated according to the amounts of SCOD removed, assuming a biomass yield of 1.0 g $COD_{biomass} \cdot g$ $COD_{removed}^{-1}$) and considering that acetate was the predominant VFA (with negligible VFA uptake by acetogens) (Hülsen et al., 2014). Considering the high concentration of solids in the FPPBR influent, it was difficult to differentiate between the volatile solids from PPB biomass, other bacteria, and the wastewater itself. Therefore, on the one hand the measured values overestimate the productivities corresponding to PPB biomass and, on the other, the estimated productivities assume that no solids are degraded and eventually transformed into PPB biomass, which underestimates the PPB-biomass productivities (note fermenter effluent contains ~1.0 g $VS \cdot L^{-1}$, Table 1). Nevertheless, both values are useful, as the measured productivities correspond to the biomass that would be harvested in large-scale installations (*e.g.*, via centrifuge), and the estimated values correspond to the “minimum” achieved productivities, which are useful for the comparison between the different operational phases.

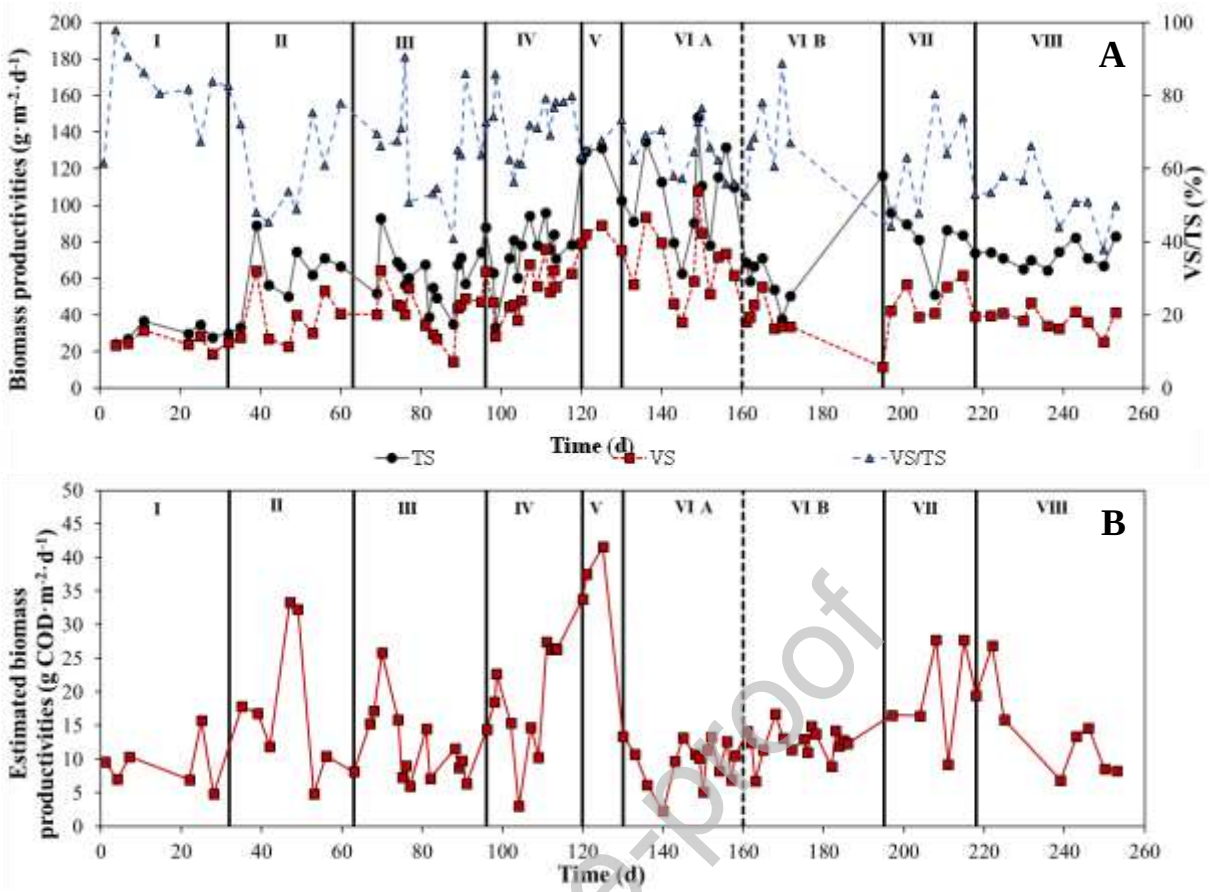

Figure 3. (A) Experimental biomass productivities and (B) PPB biomass productivities estimated from the measured SCOD consumption (assuming a biomass yield of 1 g $COD_{biomass}$·g $COD_{removed}^{-1}$). The roman numbers refer to the phases described in Table 2 (Phase I: fed continuously with FWW; Phases II-III: influent changed to FDAF; Phase IV: HRT decreased to 1 d; Phase V: HRT increased to 2.4 d and feeding only during daytime; Phases VI-VIII: aeration provided during night-time).

Depending on the reactor operation (*e.g.*, HRT), the environmental conditions and the wastewater characteristics, the measured biomass productivities ranged between 14-107 g $VS·m^{-2}·d^{-1}$. The average values for each phase (Table 3) ranged between 25-84 g $VS·m^{-2}·d^{-1}$. These estimated productivities (based on SCOD removal) were substantially lower (average values of 6.0-24 g $VS·m^{-2}·d^{-1}$, assuming a conversion ratio of 1.6 g $COD·g\ VS^{-1}$), clearly indicating the impact of the influent solids load. The latter values are similar to those

previously reported for indoor, continuously illuminated PPB lab systems (Alloul et al., 2021; Delamare-Debouteville et al., 2019; Hülsen et al., 2018b). These results are also similar to common microalgal productivities in open and closed PBRs (6.8±3.0 and 9.3±2.0 g $TS \cdot m^{-2} \cdot d^{-1}$ (Richardson et al., 2014)). While microalgae PBRs occasionally achieve higher productivities (*e.g.*, 50-60 $g \cdot m^{-2} \cdot d^{-1}$), realising 10-20 g $TS \cdot m^{-2} \cdot d^{-1}$ on an annual basis has been proven very difficult (National-Research-Council, 2012; Shen et al., 2009).

Considering that the operational period of the PPB FPPBR covered almost the entire year (only missing November and December, two very warm months in Australia, with high sunlight irradiance which would not result in a biomass productivity drop but in increased productivities), it appears realistic to generate at least 15 g $VS \cdot m^{-2} \cdot d^{-1}$ on solid free (or almost free) influents on an annual basis. This value might be used as a lower limit productivity for the economic evaluation of a large-scale plant where ~24 g $VS \cdot m^{-2} \cdot d^{-1}$ might be an upper limit (for now).

To evaluate the quality of the generated biomass, the reactor effluent was collected in an IBC with a volume of 1.0 m^3, and centrifuged. Under the applied conditions (feed flows of 6-10 $L \cdot min^{-1}$), the average biomass recovery was ~20% of the total IBC TS content (data not shown). Despite the relatively low VS/TS ratios measured in the FPPBR (40-90%, Figure 3), the VS proportion in the harvested biomass was much higher (average of 90%, Table 4). This was achieved by manually separating the “clean” biomass in the upper layer from the lower layer with heavier inerts in the centrifuge drum (also harvested for fertiliser trials). A high VS/TS ratio (>90%) is crucial for the application of the biomass as feed and, as feed trials were to be carried out using the harvested biomass, special care was taken. The CP content in the harvested biomass was 58% of the TS (CP over total VS; 49% protein content), a value in agreement with the literature and confirming the applicability of the harvested PPB biomass as potential SCP source (Capson-Tojo et al., 2020; Hülsen et al., 2018a). Furthermore, both the amino acid contents (466 $g \cdot kg^{-1}$) and the amino acid profile of the biomass (see Table S2) were acceptable as SCP, but a potential product would likely

require sterilisation. The ash content (below 10%) was within acceptable ranges for this purpose. Regarding metal contents, the Al content was notable (2,470 mg·kg^{-1}; Table 4), albeit Al containing flocculants were not used in the DAF.

Table 4. Average characteristics of the harvested biomass.

Component/characteristic	Units	Mean
TS	g·kg^{-1}	912±8.6
VS	g·kg^{-1}	822±4.4
VS/TS	%	90±0.7
TKN	g N·kg^{-1}	92±22
TP	g P·kg^{-1}	12±1.6
CP	% w/w	58±13.9
Protein	% w/w	49.2
Carbohydrates	% w/w	24.2
Fat	% w/w	17.5
Ash	% w/w	9.1
Amino acids	g·kg^{-1}	466±150
Aluminium	mg·kg^{-1}	2,470
Arsenic	mg·kg^{-1}	1.1
Cadmium	mg·kg^{-1}	0.29
Copper	mg·kg^{-1}	86
Chromium	mg·kg^{-1}	18
Iron	mg·kg^{-1}	1,330
Lead	mg·kg^{-1}	0.6
Selenium	mg·kg^{-1}	0.9
Zinc	mg·kg^{-1}	517

TS for total solids, VS for volatile solids, TKN for total Kjeldahl nitrogen, TP for total phosphorus, and CP for crude protein.

3.1.3. Microbial composition over time

The total relative abundance of PPB in the biomass from the FPPBR (direct sampling, not after centrifugation) was always over 0.20 during stable operation, with values up to 0.56

under optimal working conditions (Figure 4; the reason for the variations will be further explained in Section 3.2). These values are in agreement with data from previous studies using artificially-illuminated lab-scale reactors (Hülsen et al., 2018a, 2018b, 2016b), and with results from sunlight-illuminated PBRs fed with real wastewaters (Hülsen et al., 2022). Other than PPB, anaerobic fermenters were the most abundant organisms in the FPPBR. These bacteria were mostly grown in the fermenter (see Figure S7 for microbial communities) and, without solid/liquid separation, directly fed into the PBR. In addition, fermenters (particularly acetogens) will also grow in the FPPBR. Aerobic heterotrophs were also present in the reactor when oxygen was provided (mostly when active aeration was installed; Phases VI-VIII). Finally, fermenters and methanogens also grew in the FPPBR during periods when solids accumulation occurred, a phenomenon that was caused by improper reactor mixing (mostly during the initial operational periods, Phases I-III; see Figure S8 for the microbial compositions of samples from the bottom of the FPPBR). This issue resulted in long SRTs of the bottom fraction in the reactor, which allowed the effective growth of methanogenic archaea (Batstone et al., 2002). The mixing problems can also be observed when looking at the TCOD removal efficiencies in the FPPBR (Figure S9). The TCOD data, together with the results from overall mass balances (Table S3), show that after Phase III, the mixing system worked properly (TCOD removal stabilised around zero), with balances of COD, N, and P close to 100% (balances closed at 80-107%, 92-118%, 94-103%, respectively).

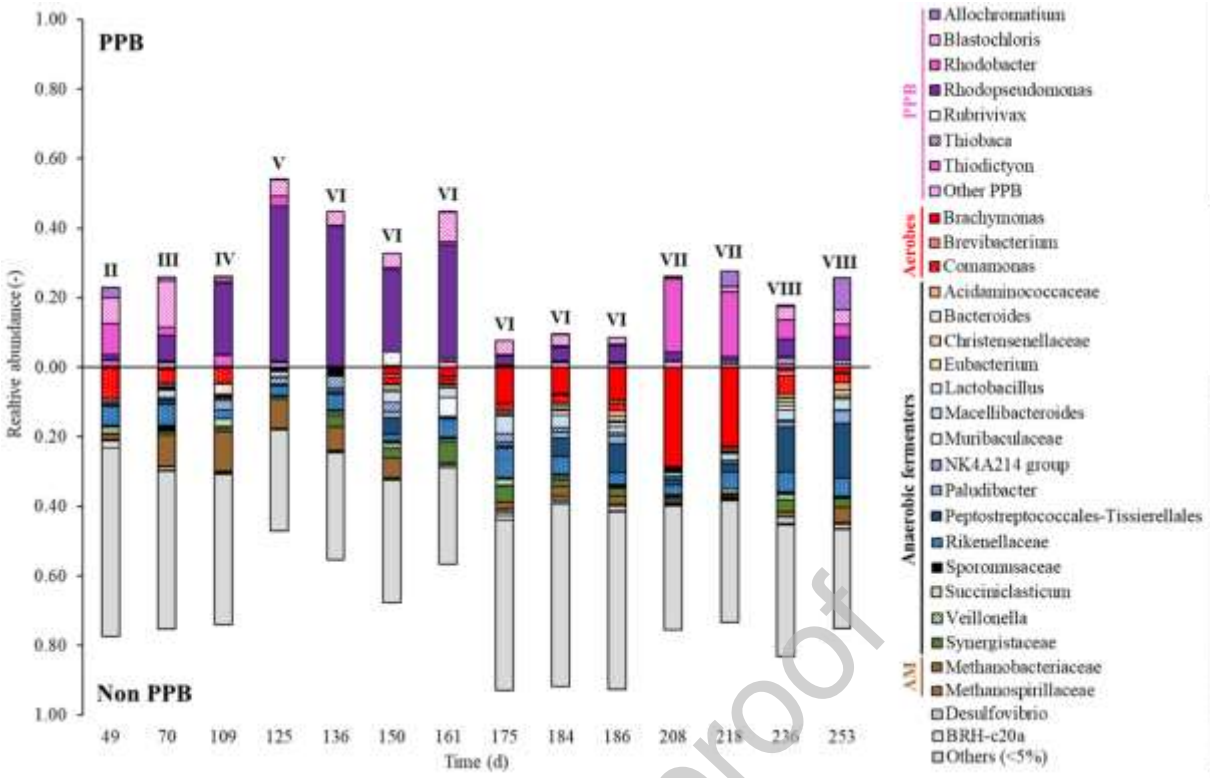

Figure 4. Microbial communities in the FPPBR during the different phases (marked by roman numbers according to Table 2 (Phase I: fed continuously with FWW; Phases II-III: influent changed to FDAF; Phase IV: HRT decreased to 1 d; Phase V: HRT increased to 2.4 d and feeding only during daytime; Phases VI-VIII: aeration provided during night-time)). AM stands for acetoclastic methanogens and PPB for purple phototrophic bacteria.

3.2. Performance during the different operational phases

3.2.1. Continuous reactor feeding: reactor influent and importance of mixing

The first phase served as start-up period and for the development of a stable microbial community. The duration of Phase I, of 32 d, ensured that a pseudo-steady state was reached (the HRT in the FPPBR was 4.4-5.7 d). The stable performance of the reactor, with removal efficiencies of VFA, TKN, and TP, of practically 100%, 70-80% and 35-52%, confirmed the proper functioning of the reactor (Figure 2). The development of a stable PPB community was further confirmed by the colour of the reactor (see Figure 1), established after only 1 week.

Although the performance of the reactor was satisfactory, the high solids content in the raw wastewater (around 3.0 g $TS \cdot L^{-1}$; see Table S1) led to solids accumulation in both the fermenter and the bottom of the FPPBR (4.7 g $TS \cdot L^{-1}$; Table S1), which led to inconsistent mass balances and a considerable apparent removal of TCOD (see Table S3 and Figure S9). During Phase II, the fermenter was fed with pretreated wastewater, after partial solid removal in an existing DAF unit (part of the wastewater treatment process at the factory), to solve this issue. This, together with modifications of the mixing system, improved the performance, and solved the issue of solid accumulation in the fermenter and reactor, particularly after Phase III (see Table S3 and Figure S9 for the corresponding TCOD removal efficiencies and mass balances).

In Phase II, the growth strategy was also changed, from suspended to attached growth, by simply letting the biofilm grow on the reactor walls and wiping the walls every 3-4 days. This was practically challenging, and made the estimation of biomass productivities difficult. From Phase III on, this approach was no longer used, and the suspended growth approach was re-applied, mechanically wiping the walls few times a day. The slightly lower removal efficiencies and higher productivities in Phase II compared to Phase I cannot directly be attributed to biofilm formation, as the HRT was also reduced to 2 d (from 4.4-5.7 d in Phase I). In fact, the performances of Phases II and III (with equal operational conditions but different growth strategy (*i.e.* attached *vs.* suspended)) were very similar in average (removal efficiencies in Phase II of 91% for VFA, 46% for TKN, and 30% for TP, and measured biomass productivities of 38 g $VS \cdot m^{-2} \cdot d^{-1}$; Table 3). This suggests that attached growth does not jeopardise the removal efficiencies nor the biomass productivities. This should be further investigated, as attached and suspended growth operation provide different advantages.

In Phase III, stable, continuous operation was achieved at an HRT of 2 d initially. Efficient removal of VFAs was achieved (up to 100%), with biomass productivities up to 60 g $VS \cdot m^{-2} \cdot d^{-1}$ (estimated values of up to 25 g $VS \cdot m^{-2} \cdot d^{-1}$). Nevertheless, as aforementioned, malfunctioning of the mixing system still resulted in solid accumulation during this phase,

which eventually worsened the system performance after the first half of Phase III (see Figure 2). VFA-COD removal efficiencies dropped to 70% (days 83-117), and the VFA concentration in the effluent increased up to 292 $mg \cdot L^{-1}$. This clearly showed the relevance of a properly functioning mixing system, to enable a homogeneous reactor content, mainly to control the SRT (here SRT should equal HRT), and to minimise the growth of potential microbial competitors (*e.g.*, methanogens). Further modifications of the mixing system solved this problem, with much better mixing performances from Phase IV onwards (Table S3 and Figure S9).

With proper mixing and stable operation in place, a similar operational strategy was maintained during Phase IV, but the HRT was further decreased to 1 d, aiming to enhance the removal rates and biomass productivities. It must be considered that in continuously fed outdoors PPB reactors, the effective illuminated HRT is actually halved, as natural daily cycles limit light supply to daytime periods. The applied 1 d HRT during Phase IV (with an effective illuminated HRT of 0.5 d) resulted in a decrease of the reactor performance, with average VFA removal efficiencies going down to 67%, and with a concomitant reduction of the removal efficiencies of N and P (as VFA availability was the factor limiting nutrient removal). Therefore, it was concluded that, while an HRT of 2 d (1 d of illuminated HRT) was effective (early Phase III), further HRT reduction to 1 d (0.5 illuminated) resulted in a performance decrease due to biomass washout (PPB growth rates of around 2.4 d^{-1} at 20-25 ºC have been reported for enriched cultures (Puyol et al., 2017)). Therefore, the overall HRT was again increased in the coming phases (2.4 d in Phase V). The possibility of biomass retention (*e.g.*, using membranes, or cloth filtration as a cheaper alternative) could solve this problem, as biomass retention can reduce the applicable HRTs by increasing the biomass concentration. However, this will also create additional problems of shading and IR attenuation and requires further research, outdoors and at scale.

3.2.2. Continuous vs. discontinuous anaerobic-illuminated operation

Despite the generally satisfactory performance during the continuously fed phases (*i.e.*,

Phases I-IV; complete VFA removal achieved in Phases I-III), daily cycle studies revealed the main issue of this approach: the lack of light during night-time naturally resulted in a pause of phototrophic activity, which lead to the discharge of basically untreated wastewater (especially at low HRTs). The results from daily cycle studies performed during Phases II and III illustrate this issue (Figure 5). The lack of light resulted in increasing SCOD and VFA concentrations during the night (fermentation), which in turn lead to a pH drop. The same behaviour was observed in all the cycles studies carried out during these periods (see Figure S10).

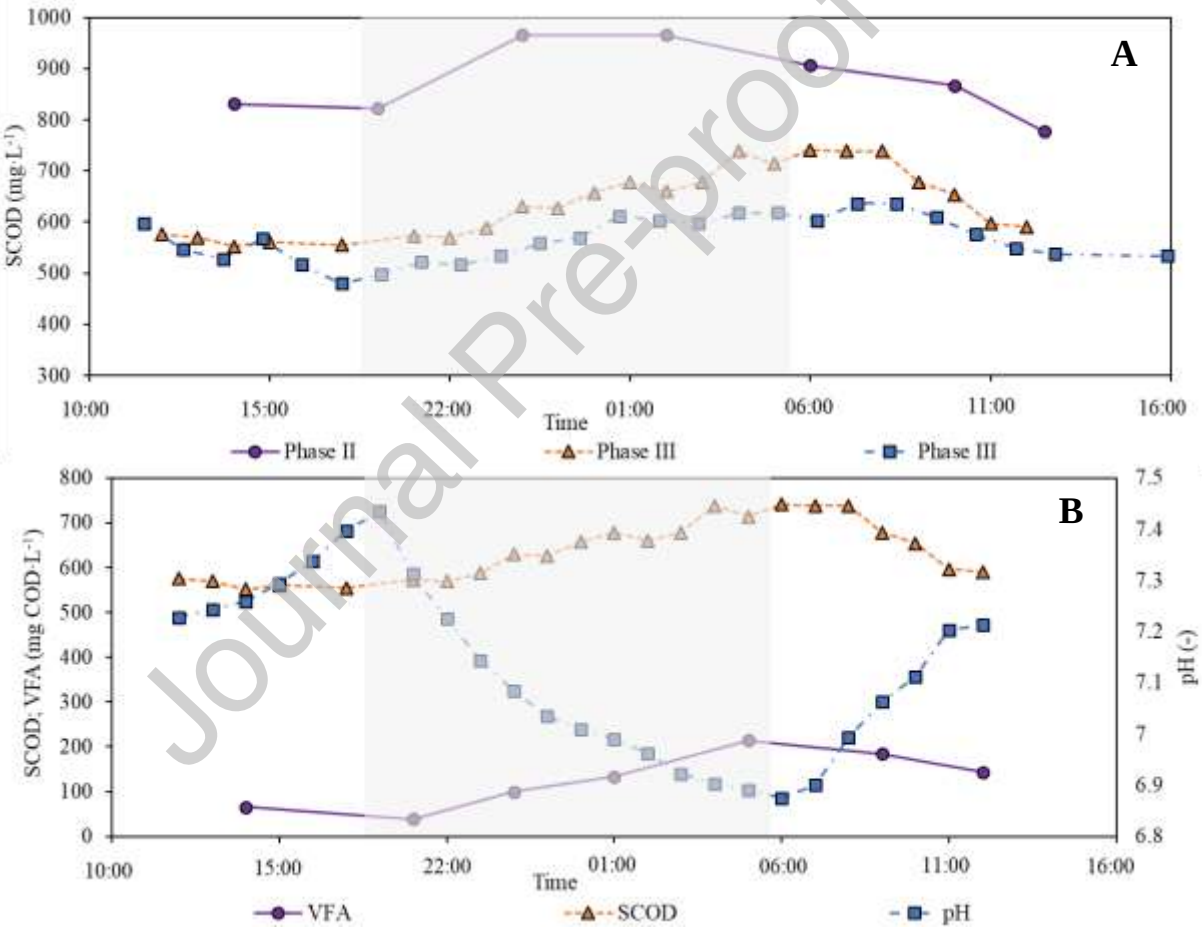

Figure 5. (A) SCOD curves during the daily cycle studies carried out during Phases II-III (fed continuously). (B) VFA, SCOD and pH profiles in the first daily cycle study from Phase III. Night hours are represented by grey-shaded areas.

To solve this problem, the feeding strategy in Phase V was changed from continuous feeding to semi-continuous feeding, only during daytime hours. The overall HRT during this phase was 2.4 d HRT, meaning that the effective-illuminated HRT was 1.2 d (the reactor was only fed during daytime). This strategy resulted in a less pronounced VFA accumulation and pH drop during the night (see Phase VI daily cycle study in Figure 6). In addition, this modification clearly enhanced the performance of the FPPBR, with VFA removal efficiencies over 95% (TKN removal efficiencies ~58% and TP ~30%, again depending of the fermenter performance and the COD:N:P ratio of the substrate; Figure 2), and much higher biomass productivities than those achieved previously (average values of 84 g $VS \cdot m^{-2} \cdot d^{-1}$ (measured) and 24 g $VS \cdot m^{-2} \cdot d^{-1}$ (estimated) *vs.* values of 41 and 12 g $VS \cdot m^{-2} \cdot d^{-1}$ in Phase III, with the same overall HRT. The highest productivities in this study were achieved during this period, with maximum values of 107 and 42 g $VS \cdot m^{-2} \cdot d^{-1}$ (measured and estimated, respectively). In addition, feeding only during the day resulted in doubled PPB relative abundances compared to previous phases (from 0.23-0.26 in Phases II-IV to 0.54 in Phase V; Figure 4). These results clearly show that operation of the FPPBR at an illuminated HRT of 1.2 d is feasible.

Several reasons can explain the improved performances when feeding only during daytime. First of all, this avoided the discharge of untreated effluent (while maintaining similar overall HRTs to those working under continuous feeding, *i.e.*, 2 d in Phase III). This also minimised the accumulation of VS during the night, and favoured fermentation of residual organic matter, which are available for PPB at the first sunbeams. Secondly, as rapidly degradable COD (such as VFA) was only available during daytime (period when PPB were dominant due to sunlight), PPB had a competitive advantage over non-phototrophic organisms, such as methanogens (if solids accumulation occurs), aerobes that might grow if residual oxygen is present, or acetogenic anaerobes. Indeed, the increase in PPB relative abundance in Phase V was at the expense of aerobic heterotrophs, anaerobic fermenters, and methanogens (Figure 4). Thirdly, seasonal factors might play a role, noting that Phase V occurred during

April and May (Australian autumn), corresponding to some of the lowest recorded irradiances and temperatures (outside and in the reactor, see Figures S5 and S6), suggesting that these aspects were not limiting the FPPBR performance.

We further note that even at low VFA-COD concentrations in the effluent, the SCOD content was on average 726 mg COD·L^{-1} during Phases I-V, with 574 mg COD·L^{-1} corresponding to non-VFA SCOD (reason why there is a SCOD baseline in Figure 5). The nature of this non-biodegradable SCOD was not elucidated, but we suspect non-degradable residues from, for example, the feather stream, and exclude products from PPB degradation. This is underlined by a similar non-degradable SCOD fraction in the fermenter effluent during Phase V (average non-VFA SCOD of 488 mg·L^{-1} from a total SCOD of 1,260 mg COD·L^{-1}; see baseline in Figure S3) as well as non-degraded filtered TKN.

3.2.3. Combined anaerobic-illuminated/aerobic-dark operation

To enhance the wastewater treatment performance during night hours, we aimed to exploit the metabolic versatility of PPB by supplying oxygen during night-time. It has been demonstrated that the oxidative conditions resulting from the presence of oxygen result in the suppression of photoheterotrophic growth and in the out-competition of PPB if oxygen supply is continuous (Capson-Tojo et al., 2021). Nevertheless, the aerobic capabilities of PPB give them some resilience, which opens the door for a mixed metabolic mode (3MPPB) operation, exploiting PPBs photoheterotrophic metabolism under anaerobic illuminated conditions during the day (PhAnI), and chemoheterotrophy of the same PPB, under aerobic, dark conditions (at night) (ChAerD). The 3MPPB approach was tested in Phases VI-VIII, aiming to extend PPB treatment from the day to the night by continuing to remove COD and thus avoiding VFA accumulation during night-time. During Phase VI A, initial pulsed aeration through a perforated pipe from day 130 to day 160 (9/16 min ON/OFF at 62.3 L·min^{-1}) did not result in continuously measurable DO (Figure S6). After day 160, Phase VI B, the aeration was supplied continuously, resulting in a substantial increase in the DO concentrations (up to saturation levels in some days (Figure S6)). This means that Phase VI A was mostly

anaerobic until day 160 (with some DO spikes at night). The corresponding cycle study was performed before day 160, and the trends corresponding to Phase VI A (Figure 6) therefore represent an anaerobic system. The SCOD and VFA in Phase VI increased slightly in the dark, with a concomitant pH drop, even without feeding at night, resembling, albeit to a lower extent, the trends of Figure 5 (Phases II-III). These trends were related to the hydrolysis and fermentation of complex organics already present in the reactor. In fact, the performances, microbial communities, and measured biomass productivities were very similar between Phase V and Phase VI A (Figures 2, 3 and 4; the estimated productivities were different due to failures in the fermenter during the beginning of Phase VI).

From Phase VII, DO was controlled using a dedicated PLC and flexible air diffusers to increase the oxygen transfer efficiency. This resulted in effective aeration during night-time and in a reduction of the SCOD concentrations during the night, enhancing the quality of the discharged effluent. Night aeration not only avoided SCOD accumulation, but also reduced the SCOD baseline from around 700 mg $COD \cdot L^{-1}$ down to 320-410 mg $COD \cdot L^{-1}$. This suggests that the biodegradable extent of the influent COD was enhanced under aerobic conditions. Indeed, the highest SCOD, TKN and TP removal efficiencies using fermented DAF effluent were reported during Phase VII (67%, 53%, and 45%, respectively). This confirms the positive effect of oxygen supply on the system performance, at least in terms of pollutant removal and discharge savings. This operation also circumvented the pH drop observed during strictly anaerobic operation (Figure S6C). The same behaviour was observed in a cycle study from Phase VII (Figure S11).

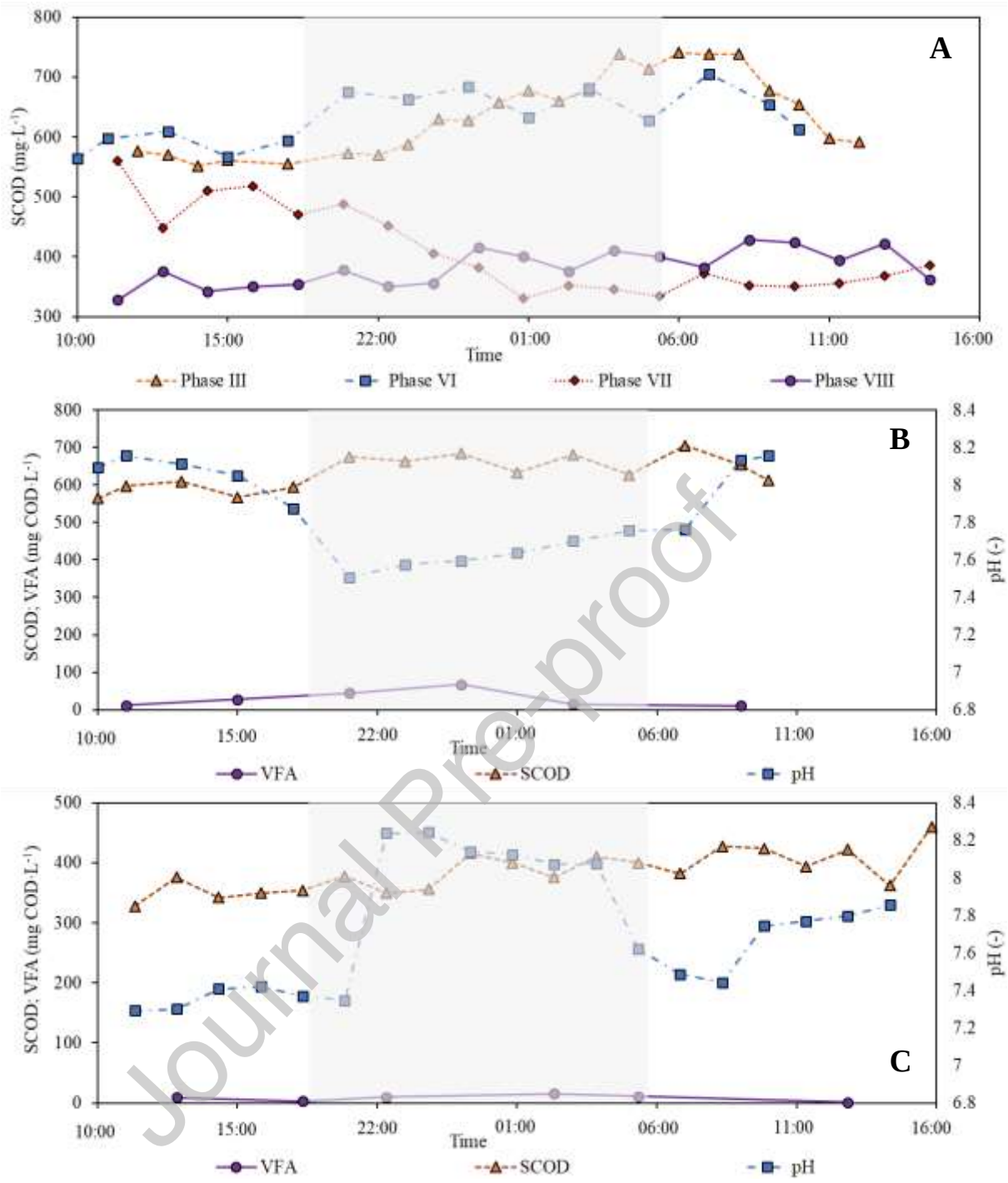

Figure 6. (A) SCOD curves during the daily cycle studies carried out during Phase III (anaerobic) and Phases VI-VIII (aerated during night-time). VFA, SCOD and pH profiles in the daily cycle study from (B) Phase VI and (C) Phase VIII.

The enhanced performance observed in Phases VII-VIII was not observed in Phase VI. As aforementioned, the operation during the first half of Phase VI A (until day 160) was

practically anaerobic, as the air supply did not result in increased DO concentrations in the reactor, nor SCOD removal at night. After this phase, the increasing DO concentrations resulted in a sudden reduction in the PPB relative abundances (from 0.45 on day 161 to 0.08 in day 175; Figure 4). This was accompanied by a decrease in the measured biomass productivities, from 55 g $VS \cdot m^{-2} \cdot d^{-1}$ on day 165 down to 34 g $VS \cdot m^{-2} \cdot d^{-1}$ in days 170-172 (most likely related to the lower biomass yields of other bacteria compared to PPB growing photoheterotrophically). The decrease in PPB proportions can be observed in Phases VI-VIII (Figure 4). At the beginning of Phase VI, the relative abundance of PPB was above 50% with *Rhodopseudomonas sp.* accounting for over 70% of the total PPB in all the samples (days 125, 136, 150 and 161). After implementing continuous aeration (in day 160), the PPB community collapsed to relative abundances below 10%, clearly caused by the condition change (day 175). Unfortunately, there was an accidental NaOH addition between days 183-189 into the wastewater, which led to a sharp increase in the reactor pH (average daily value of 10.5) and reactor failure.

Because of this, the reactor was restarted on day 192, using 100 L of an enriched PPB culture from a backup reactor as starting inoculum. The PPB community dynamics remain unclear, as *Rhodobacter sp.* dominated after the restart with over 67% of the total PPB in Phase VII (Figure 4, days 208, 218). A redistribution of PPB representatives in Phase VIII, makes us believe that *Rhodopseudomonas sp.* might have re-emerged, given more time. At this stage, we cannot state that the shift from a *Rhodopseudomonas*-dominated system (anaerobically) to a *Rhodobacter*-dominated reactor community was caused by aeration. Similar redistributions were observed in other publications, especially after shocks such as aeration (Hülsen et al., 2019) and parameter change (*e.g.*, SRT) (Alloul et al., 2019; Hülsen et al., 2020).

While we cannot make claims around the events in Phase VI, based on the following Phases VII and VIII it becomes evident that PPB can be maintained in a 3MPPB concept. These phases were characterised by enhanced wastewater treatment capabilities under night-

aeration operation, with lower overall PPB abundance compared to purely anaerobic operation, down to 0.2-0.3 in Phases VII-VIII (*vs.* over 0.5 in Phase V or the beginning of Phase VI; Figure 4). This is a consequence of aerobic chemoheterotrophic growth of PPB and non-phototrophic aerobes during night-time (biomass yields around 0.5 g COD·g COD^{-1}), with the latter representing up to 28% of the microbial population in Phase VII (Figure 4). Reducing the HRT in Phase VIII to 1.6 d helped to minimise the presence of aerobic heterotrophs, but did not result in increased PPB proportions, as PPB were also washed out. The system would benefit from biomass retention to separate the HRT from the SRT, so HRT/SRT control is not the way to control common aerobes. Oxygen control appears as the way forward, but the success depends on the substrate affinities of PPB *vs.* common aerobes. More research is required to optimise the system during night-time, which also requires an understanding of the underlying biological mechanisms.

Finally, during night-time aeration the HRT was reduced from 2.1 d in Phase VII to 1.6 d in Phase VIII (illuminated HRT of 0.8 d). The reactor performed properly, but lower VFA removal efficiencies were obtained (67-100%). Furthermore, the reduction of the HRT did lower the removal efficiencies, the PPB proportions, and did not increase the biomass productivities (see Table 3 and Figure 4). Therefore, if biomass retention is not provided, we recommend a minimum overall HRT of 2-2.4 d (illuminated HRT of 1-1.2 d).

3.3. Implications for industrial application

This work describes a modular, scalable FPPBR for PPB mediated wastewater treatment and resource recovery in the form of PPB biomass. The reactor was functional, removing almost all the VFA in the influent at rates around 0.5 g SCOD·L^{-1}·d^{-1}, with peaks up to 1.0 g SCOD ·L^{-1}·d^{-1}. This was achieved without biomass retention in a flowthrough system at total HRTs (equal to SRT) of 1.6-2.4 d (or illuminated HRTs of 0.8-1.2 d). The OLR can theoretically be higher, but the effects on the pH have to be considered, particularly if feeding fermented wastewater (*i.e.*, reduced pH due to high VFA concentrations will inhibit PPB). In subtropical regions, at a light path of 40 mm (80 mm reactor width), the PBR effluent had TS

concentrations of around 1.5-2.0 $g \cdot L^{-1}$ (with up to 50% of native solids from the wastewater). This resulted in estimated (conservative estimates, not measured values) biomass productivities between 6.0-24 g $VS \cdot m^{-2} \cdot d^{-1}$, where 24 g $VS \cdot m^{-2} \cdot d^{-1}$ were achieved during stable operation in the Australian autumn, at a low light intensity and low temperature period. In consideration of the underestimation of this productivity (as explained above), we take this value as a conservative estimate of realisable biomass production throughout the year (corresponding to 504 g $VS \cdot m^{-3} \cdot d^{-1}$). For poultry processing wastewater, the corresponding COD, VFA-COD, TN and TP removal efficiencies were around 67±12, 87±7.5, 53±0 and 45±6.0, respectively (*e.g.*, Phase VII). For mixed anaerobic (day) and aerobic (night) operation in a 3MPPB system, additional aeration costs will occur (*e.g.*, to realise 0.1 mg $DO \cdot L^{-1}$ during the night). The latter depends on the standard oxygen transfer efficiency of the aerators and the height of the water column, here around 900 mm. A detailed economic analysis including the capital costs of a scaled plant must be done in a follow up study.

This study has shown that the reactor operation is robust and that it can handle temperature and irradiance fluctuations throughout the year. This includes day and night temperature fluctuations of up to 24°C, with peak lows of 6.0°C and peak highs over 45°C, confirming results from lab studies (Hülsen et al., 2016a) and a recent outdoor study (Hülsen et al., 2022). The system was operated without a PLC and did not require detailed controls (expect for the latter phases where DO concentration was controlled). However, for prefermented wastewater as feed, pH control is desirable, and for aeration at night, a DO sensor would optimise the oxygen supply. Without the aerobic step at night, the PPB plant performance is limited to a semi-continuous feed regime during daytime hours. The 3MPPB concept might enable continuous day and night operation at higher OLR and higher volumetric conversions but the microbial competition has to be determined. The overall resource recovery would likely be reduced due to lower biomass yields under predominant chemoheterotrophic growth (Tchobanoglous et al., 2003). The latter would depend on the volumetric conversion at night relative to the conversion during the day. More research is required to assess this option and

its effects on the microbial community. However, we showed that effluent polishing is feasible. Nevertheless, this approach requires an aeration system and strict microbial community control. The cost-benefit comparison has to be made to evaluate this concept.

One major option to enhance the reactor performance in strict anaerobic or in mixed metabolic mode, is to provide biomass retention via membranes or cloth filtration, which has the potential to increase the PPB biomass in the reactor and increase the volumetric and areal removal efficiencies and productivities, while shortening the HRTs. This has to be combined with continuous harvesting of biomass from the reactor to maintain a SRT of 2-4 d (Hülsen et al., 2018b, 2016b). This will also impact the light supply, via increased shading and light attenuation of the infrared light, which requires detailed analysis. The options of attached biofilm or even the use of PPB granules (Stegman et al., 2021) are perceivable, but require more research.

From this work, we can further outline some major differences of FPPBRs for algal and PPB biomass production. For strictly anaerobic operation (photoheterotrophy), a PPB FPPBR does not require a distribution system for CO_2 supply and O_2 stripping (no product inhibition). A PPB FPPBR does likely not require cooling or heating (subject to local conditions) and the impact of (aerobic) grazers can be neglected. Another argument is the doubling of the light path (relative to a pond), due to two sided light supply, which should enable less shading, higher biomass concentrations, higher volumetric removal and productivities. Biomass productivity is further independent from CO_2 supply, as COD in a secondary treatment step is the main driver for N and P removal. In combination with lower light requirements of PPB, this might result in higher annual productivities, especially on VFA rich wastewaters (*e.g.*, after prefermentation).

Theoretically, PPB can be used to treat any wastewater with sufficient bioavailable COD, as shown in several publications (Capson-Tojo et al., 2020). As presented here, this includes wastewater with fats, proteins, or other (inert) solids, which, however, might affect the biomass quality and its use as valuable product (*e.g.*, SCP as feed). The here achieved

results can be extrapolated to other wastewaters, especially easy degradable wastewater *e.g.*, from food processing, which would likely result in improved performances. Finally, the PPB biomass was tested as fish and prawn feed, where up to 66% and 100% of fishmeal in commercial feed have been successfully substituted with PPB biomass (Delamare-Deboutteville et al., 2019) (prawn feed data are not published at the moment). Fertiliser trials were also performed on various crops (data not shown). The product testing further enables addition of a potential price tag on the biomass, which can be used for economic feasibility studies, which will be key to evaluate the viability of this technology.

4. Conclusions

The PPB demonstration plant provided consistent performance (*i.e.*, removal efficiencies of VFAs, TKN, and TP of >90%, 34-77%, and 28-45%) and estimated (conservative) biomass productivities of 6-24 g $VS \cdot m^{-2} \cdot d^{-1}$, under varying wastewater characteristics and environmental conditions. The removal of N and P was limited by the availability of biodegradable COD, a property of the feed wastewater. The harvested biomass had a VS/TS ratio over 90%, a CP content of 58%, and a compatible amino acid profile. On average, the FPPBR showed average biomass productivities of ~15 g $VS \cdot m^{-2} \cdot d^{-1}$ and SCOD removal rates >500 $mg \cdot L^{-1} \cdot d^{-1}$, working at an HRT of 2.4 d and with semicontinuous/day-only feeding. Under these conditions, the relative abundance of PPB was 0.56. During continuous (day-night) feeding, VFA peaked during the night, particularly at low retention times. A minimum overall HRT of 1.6-2.4 d is recommended to avoid PPB washout. Finally, a combined daily-illuminated-anaerobic/night-aerobic operation (supplying air during night-time), called the 3MPPB concept, improved the removal performances, avoiding VFA accumulation (and a concomitant pH drop) during the night. Nevertheless, this approach resulted in lower PPB abundances and biomass productivities and would add extra infrastructure and operational costs.

Acknowledgements

Tim Hülsen is grateful to The Queensland Government, GHD, Ridley, Aquatec Maxcon and Ingham for their financial support as part of an Advanced Queensland Industry Fellowship. The authors also acknowledge the support of Meat and Livestock Australia through their funding from the Australian Government Department of Agriculture, Water and the Environment, as part of its Rural R&D for Profit program. Gabriel Capson-Tojo wants to acknowledge the Xunta de Galicia for his postdoctoral fellowship (ED481B-2018/017).

*Declaration of Interest Statement

none

References

Acién, F.G., Molina, E., Fernández-Sevilla, J.M., Barbosa, M., Gouveia, L., Sepúlveda, C., Bazaes, J., Arbib, Z., 2017. Economics of microalgae production. Microalgae-Based Biofuels Bioprod. From Feed. Cultiv. to End-Products 485–503. https://doi.org/10.1016/B978-0-08-101023-5.00020-0

Adessi, A., Torzillo, G., Baccetti, E., De Philippis, R., 2012. Sustained outdoor H2 production with Rhodopseudomonas palustris cultures in a 50 L tubular photobioreactor. Int. J. Hydrogen Energy 37, 8840–8849. https://doi.org/10.1016/j.ijhydene.2012.01.081

Alloul, A., Cerruti, M., Adamczyk, D., Weissbrodt, D.G., Vlaeminck, S., 2021. Operational Strategies to Selectively Produce Purple Bacteria for Microbial Protein in Raceway Reactors. Environ. Sci. Technol. 55, 8278–8286. https://doi.org/https://doi.org/10.1021/acs.est.0c08204

Alloul, A., Wuyts, S., Lebeer, S., Vlaeminck, S.E., 2019. Volatile fatty acids impacting phototrophic growth kinetics of purple bacteria: Paving the way for protein production on fermented wastewater. Water Res. 152, 138–147.

https://doi.org/10.1016/j.watres.2018.12.025

APHA, 2005. Standard Methods for the Examination of Water and Wastewater. American Public Health Association, Washington, DC.

Batstone, D.J., Keller, J., Angelidaki, I., Kalyuzhny, S. V, Pavlostathis, S.G., Rozzi, A., Sanders, W.T.M., Siegrist, H., Vavilin, V.A., 2002. Anaerobic digestion model no. 1 (ADM1). IWA Publishing. https://doi.org/https://doi.org/10.2166/wst.2002.0292

Benemann, J.R., Woertz, I., Lundquist, T., 2018. Autotrophic microalgae biomass production: from niche markets to commodities. Ind. Biotechnol. 14, 3–10.

Bolger, A.M., Lohse, M., Usadel, B., 2014. Trimmomatic: A flexible trimmer for Illumina sequence data. Bioinformatics 30, 2114–2120. https://doi.org/10.1093/bioinformatics/btu170

Caporaso, J.G., Kuczynski, J., Stombaugh, J., Bittinger, K., Bushman, F.D., Costello, E.K., Fierer, N., Peña, A.G., Goodrich, J.K., Gordon, J.I., Huttley, G.A., Kelley, S.T., Knights, D., Koenig, J.E., Ley, R.E., Lozupone, C.A., Mcdonald, D., Muegge, B.D., Pirrung, M., Reeder, J., Sevinsky, J.R., Turnbaugh, P.J., Walters, W.A., Widmann, J., Yatsunenko, T., Zaneveld, J., Knight, R., 2010. QIIME allows analysis of high- throughput community sequencing data Intensity normalization improves color calling in SOLiD sequencing. Nat. Methods 7, 335–336. https://doi.org/10.1038/nmeth0510-335

Capson-Tojo, G., Batstone, D.J., Grassino, M., Vlaeminck, S.E., Puyol, D., Verstraete, W., Kleerebezem, R., Oehmen, A., Ghimire, A., Pikaar, I., Lema, J.M., Hülsen, T., 2020. Purple phototrophic bacteria for resource recovery: Challenges and opportunities. Biotechnol. Adv. 43, 107567. https://doi.org/doi.org/10.1016/j.biotechadv.2020.107567

Capson-Tojo, G., Lin, S., Batstone, D.J., Hülsen, T., 2021. Purple phototrophic bacteria are outcompeted by aerobic heterotrophs in the presence of oxygen. Water Res. 194, 116941. https://doi.org/10.1016/j.watres.2021.116941

Carlozzi, P., Pushparaj, B., Degl'Innocenti, A., Capperucci, A., 2006. Growth characteristics of Rhodopseudomonas palustris cultured outdoors, in an underwater tubular

photobioreactor, and investigation on photosynthetic efficiency. Appl. Microbiol. Biotechnol. 73, 789–795. https://doi.org/10.1007/s00253-006-0550-z

Carlozzi, P., Sacchi, A., 2001. Biomass production and studies on Rhodopseudomonas palustris grown in an outdoor, temperature controlled, underwater tubular photobioreactor. J. Biotechnol. 88, 239–249. https://doi.org/10.1016/S0168-1656(01)00280-2

Chitapornpan, S., Chiemchaisri, C., Chiemchaisri, W., Honda, R., Yamamoto, K., 2013. Organic carbon recovery and photosynthetic bacteria population in an anaerobic membrane photo-bioreactor treating food processing wastewater. Bioresour. Technol. 141, 65–74. https://doi.org/10.1016/j.biortech.2013.02.048

Dalaei, P., Bahreini, G., Nakhla, G., Santoro, D., Hülsen, T., 2020. Municipal wastewater treatment by purple phototropic bacteria at low infrared irradiances using a photo-anaerobic membrane bioreactor. Water Res. 115535. https://doi.org/10.1016/j.watres.2020.115535

Day, J.G., Gong, Y., Hu, Q., 2017. Microzooplanktonic grazers – A potentially devastating threat to the commercial success of microalgal mass culture. Algal Res. 27, 356–365.

Delamare-Deboutteville, J., Batstone, D.J., Kawasaki, M., Stegman, S., Salini, M., Tabrett, S., Smullen, R., Barnes, A.C., Hülsen, T., 2019. Mixed culture purple phototrophic bacteria is an effective fishmeal replacement in aquaculture. Water Res. X 4, 100031. https://doi.org/10.1016/j.wroa.2019.100031

Edgar, R.C., 2010. Search and clustering orders of magnitude faster than BLAST. Bioinformatics 26, 2460–2461. https://doi.org/10.1093/bioinformatics/btq461

Eding, E.H., Kamstra, A., Verreth, J.A.J., Huisman, E.A., Klapwijk, A., 2006. Design and operation of nitrifying trickling filters in recirculating aquaculture: A review. Aquac. Eng. 34, 234–260. https://doi.org/10.1016/j.aquaeng.2005.09.007

Engelbrektson, A., Kunin, V., Wrighton, K.C., Zvenigorodsky, N., Chen, F., Ochman, H., Hugenholtz, P., 2010. Experimental factors affecting PCR-based estimates of microbial

species richness and evenness. ISME J. 4, 642–647. https://doi.org/10.1038/ismej.2009.153

Hülsen, T., Barry, E.M., Lu, Y., Puyol, D., Batstone, D.J., 2016a. Low temperature treatment of domestic wastewater by purple phototrophic bacteria: Performance, activity, and community. Water Res. 100, 537–545. https://doi.org/10.1016/j.watres.2016.05.054

Hülsen, T., Barry, E.M., Lu, Y., Puyol, D., Keller, J., Batstone, D.J., 2016b. Domestic wastewater treatment with purple phototrophic bacteria using a novel continuous photo anaerobic membrane bioreactor. Water Res. 100, 486–495. https://doi.org/10.1016/j.watres.2016.04.061

Hülsen, T., Batstone, D.J., Keller, J., 2014. Phototrophic bacteria for nutrient recovery from domestic wastewater. Water Res. 50, 18–26. https://doi.org/10.1016/j.watres.2013.10.051

Hülsen, T., Hsieh, K., Batstone, D.J., 2019. Saline wastewater treatment with purple phototrophic bacteria. Water Res. 160, 259–267. https://doi.org/10.1016/j.watres.2019.05.060

Hülsen, T., Hsieh, K., Lu, Y., Tait, S., Batstone, D.J., 2018a. Simultaneous treatment and single cell protein production from agri-industrial wastewaters using purple phototrophic bacteria or microalgae – A comparison. Bioresour. Technol. 254, 214–223. https://doi.org/10.1016/j.biortech.2018.01.032

Hülsen, T., Hsieh, K., Tait, S., Barry, E.M., Puyol, D., Batstone, D.J., 2018b. White and infrared light continuous photobioreactors for resource recovery from poultry processing wastewater – A comparison. Water Res. 144, 665–676. https://doi.org/10.1016/j.watres.2018.07.040

Hülsen, T., Sander, E.M., Jensen, P.D., Batstone, D.J., 2020. Application of purple phototrophic bacteria in a biofilm photobioreactor for single cell protein production: Biofilm vs suspended growth. Water Res. 181, 115909. https://doi.org/10.1016/j.watres.2020.115909

Hülsen, T., Stegman, S., Batstone, D.J., Capson-Tojo, G., 2022. Naturally illuminated photobioreactors for resource recovery from piggery and chicken-processing wastewaters utilising purple phototrophic bacteria. Water Res. In Press, 118194.

López-Serna, R., García, D., Bolado, S., Jiménez, J.J., Lai, F.Y., Golovko, O., Gago-Ferrero, P., Ahrens, L., Wiberg, K., Muñoz, R., 2019. Photobioreactors based on microalgae-bacteria and purple phototrophic bacteria consortia: A promising technology to reduce the load of veterinary drugs from piggery wastewater. Sci. Total Environ. 692, 259–266. https://doi.org/10.1016/j.scitotenv.2019.07.126

Masella, A.P., Bartram, A.K., Truszkowski, J.M., Brown, D.G., Neufeld, J.D., 2012. PANDAseq: PAired-eND Assembler for Illumina sequences. BMC Bioinformatics 13, 1–7.

National-Research-Council, 2012. Sustainable Development of Algal Biofuels in the United States. Washington DC.

Patton, C.J., Truitt, E.P., 1992. Methods of Analysis By the U.S. Geological Survey National Water Quality Laboratory—Determination of Total Phosphorus By a Kjeldahl Digestion Method and an Automated Colorimetric Finish That Includes Dialysis. U.S. Geol. Surv. Open-File Rep. 92-146.

Pearson, W.R., Wood, T., Zhang, Z., Miller, W., 1997. Comparison of DNA sequences with protein sequences. Genomics 46, 24–36. https://doi.org/10.1006/geno.1997.4995

Puyol, D., Barry, E.M., Hülsen, T., Batstone, D.J., 2017. A mechanistic model for anaerobic phototrophs in domestic wastewater applications: Photo-anaerobic model (PAnM). Water Res. 116, 241–253. https://doi.org/10.1016/j.watres.2017.03.022

Quast, C., Pruesse, E., Yilmaz, P., Gerken, J., Schweer, T., Yarza, P., Peplies, J., Glöckner, F.O., 2013. The SILVA ribosomal RNA gene database project: Improved data processing and web-based tools. Nucleic Acids Res. 41, 590–596. https://doi.org/10.1093/nar/gks1219

Richardson, J.W., Johnson, M.D., Zhang, X., Zemke, P., Chen, W., Hu, Q., 2014. A financial

assessment of two alternative cultivation systems and their contributions to algae biofuel economic viability. Algal Res. 4, 96–104. https://doi.org/10.1016/j.algal.2013.12.003

Saer, R.G., Blankenship, R.E., 2017. Light harvesting in phototrophic bacteria: Structure and function. Biochem. J. 474, 2107–2131. https://doi.org/10.1042/BCJ20160753

Shen, Y., Yuan, W., J. Pei, Z., Wu, Q., Mao, E., 2009. Microalgae Mass Production Methods. Trans. ASABE 52, 1275–1287.

Stegman, S., Batstone, D.J., Rozendal, R., Jensen, P.D., Hülsen, T., 2021. Purple phototrophic bacteria granules under high and low upflow velocities. Water Res. 190, 116760. https://doi.org/10.1016/j.watres.2020.116760

Taiganides, G., 1992. Pig waste management and recycling: the Singapore experience.

Tchobanoglous, G., Burton, F.L., Stensel, H.D., 2003. Wastewater Engineering. Treatment and Reuse, Fourth. ed. McGraw-Hill.